HgCdTe Growth on (552) Oriented CdZnTe by Metalorganic Vapor Phase Epitaxy

P. MITRA,[1] F.C. CASE,[1] H.L. GLASS,[2] V.M. SPEZIALE,[2] J.P. FLINT,[2] S.P. TOBIN,[3] and P.W. NORTON[3]

1.—Lockheed Martin Missiles and Fire Control–Dallas, P.O. Box 650003, Dallas, TX 75265-0003. 2.—Honeywell Electronic Materials, 15128 E. Euclid Avenue, Spokane, WA 99216. 3.—BAE SYSTEMS, 2 Forbes Road, Lexington, MA 02421-7306

We report the growth of HgCdTe on (552)B CdZnTe by metalorganic vapor phase epitaxy (MOVPE). The (552) plane is obtained by 180° rotation of the (211) plane about the [111] twist axis. Both are 19.47 degrees from (111), but in opposite directions. HgCdTe grown on the (552)B-oriented CdZnTe has a growth rate similar to the (211)B, but the surface morphology is very different. The (552)B films exhibit no void defects, but do exhibit ~40 μm size hillocks at densities of 10–50 cm^{-2}. The hillocks, however, are significantly flatter and shorter than those observed on (100) metalorganic vapor phase epitaxy (MOVPE) HgCdTe films. For a 12–14 μm thick film the height of the highest point on the hillock is less than 0.75 μm. No twinning was observed by back-reflection Laue x-ray diffraction for (552)B HgCdTe films and the x-ray double crystal rocking curve widths are comparable to those obtained on (211)B films grown side-by-side and with similar alloy composition. Etch pit density (EPD) measurements show EPD values in the range of $(0.6–5) \times 10^5$ cm^{-2}, again very similar to those currently observed in (211)B MOVPE HgCdTe. The transport properties and ease of dopant incorporation and activation are all comparable to those obtained in (211)B HgCdTe. Mid-wave infrared (MWIR) photodiode detector arrays were fabricated on (552)B HgCdTe films grown in the P-n-N device configuration (upper case denotes layers with wider bandgaps). Radiometric characterization at T = 120–160 K show that the detectors have classical spectral response with a cutoff wavelength of 5.22 μm at 120 K, quantum efficiency ~78%, and diffusion current is the dominant dark current mechanism near zero bias voltage. Overall, the results suggest that (552)B may be the preferred orientation for MOVPE growth of HgCdTe on CdZnTe to achieve improved operability in focal plane arrays.

Key words: Mercury cadmium telluride, metalorganic vapor phase epitaxy (MOVPE), cadmium zinc telluride, infrared detector

INTRODUCTION

The orientation of the lattice-matched CdZnTe substrates has a profound effect on the surface morphology and the defect structure of the HgCdTe films grown by vapor phase epitaxy. In metalorganic vapor phase epitaxy (MOVPE) growth of HgCdTe, the preferred CdZnTe orientations are (100) misoriented 2–8° towards (110) or (111)B planes, and (211)B. These substrate orientations have been successfully used for the growth of high quality HgCdTe films and for the demonstration of a variety of in-situ grown p-n junction photodiode detectors as well as emitters.[1–7] The surfaces of (100)-oriented films are normally found to exhibit pyramidal hillock defects, while the (211)B-oriented films exhibit void defects.[5,8–10] Both types of macrodefects cause the photodiodes overlapping those regions to be leaky or shorted.

There have been numerous studies on the nature and causes for macro-defects on the surface of HgCdTe grown by MOVPE and their orientation dependence.[7–11] These defects nucleate on the substrate-film interface through particulates, precipitates, or due to the chemical modification of the II/VI

(Received November 25, 2000; accepted February 19, 2001)

ratio of the substrate surface induced by an etchant. On (100)-oriented GaAs substrates pre-treatment by alkaline metal containing solutions has been reported to significantly reduce the density of hillock defects on the HgCdTe epilayers.[12–14] Alternate orientations, such as the high index planes, have surfaces that can be less susceptible to macro-defect formation or the defect geometry itself may be more forgiving to the devices.

In this paper we report MOVPE interdiffused growth of HgCdTe on the (552)-oriented CdZnTe. The (552) plane is obtained by 180° rotation of the (211) plane about the [111] twist axis. The (211) and (552) planes both lie 19.47 degrees from (111), but in opposite directions. HgCdTe films grown on the (552)B-oriented CdZnTe have growth rates similar to the (211)B but the surface morphologies are very different. The (552)B films exhibit no void defects but do exhibit hillocks at densities of 10–50 cm^{-2}. The hillocks, however, are significantly flatter and smaller than those observed on (100) films of similar thicknesses. The (552)B HgCdTe film surfaces were characterized by Nomarski optical and atomic force microscopy. Epitaxial quality was assessed by x-ray diffraction and etch pit density counts. The transport properties of the n-type films were characterized by Hall effect and lifetime measurements. Mid-wave infrared (MWIR) photodiode films grown in the P-n-N configuration[6] were fabricated into back-illuminated variable-area detector arrays (here the upper case denotes layers of wider bandgaps). The detectors were tested for spectral response, quantum efficiency, current-voltage curves, and dynamic resistance-area products.

SUBSTRATES AND HgCdTe GROWTH

The (211) planes are located 19.47 degrees from (111) toward the (100). At an equal angle, but in the opposite direction, are the (552) planes. Since twins in CdZnTe can be described as having an orientation derived from the parent or matrix by a 180 degree rotation around a <111> direction, the (552) can be observed as a twinned region on a (211) wafer. In fact, our initial observation of MOVPE growth of HgCdTe on (552) was on such a twinned region that had previously gone unnoticed.

The (552) planes, like the (211), exhibit polarity associated with the nearest (111) plane. This can be revealed by the standard polarity etch[15] ($HF:HNO_3$:lactic acid in ratios 1:1:1). Etching also is commonly used to reveal defects in CdZnTe substrates. Attempts to use the defect etch developed for the (211) orientation[16] gave encouraging results. Dislocations were revealed on the B-faces, as previously identified using the polarity etch. On (552) substrates, however, dislocation etch pits were not as sharply defined as on (211). After the defect etch, the polarity of (211) substrate surfaces can be identified with the unaided eye, but microscopic examination was required to identify polarity in the (552) substrates.

MOVPE growth of HgCdTe was performed using the interdiffused process that has been previously described in detail.[5] Most of the films were grown on the (552)B face of the CdZnTe substrates. In a number of cases the films were grown side-by-side with the (211)B substrates for comparison. The growth rates on the two orientations are closely comparable, although not identical. Thus completely new calibration was not necessary to achieve comparable x-values and thicknesses. The films were typically grown to thicknesses of 9–14 μm with $Hg_{1-x}Cd_xTe$ x-values in the range of 0.21–0.40. For n-type doping the films were doped with iodine using the precursor ethyl iodide.[17] Iodine incorporation rates in the (552)B-oriented films were found to be within a factor of two of the incorporation rate in (211)B-oriented HgCdTe. This result is in marked contrast to the strong orientation dependence of the iodine incorporation observed[18] with the tilt angles between the (100) and (111) planes, but not unexpected, due to the similar structures of the (552)B and (211)B surfaces. No orientation dependence was observed for arsenic doping, which was performed with the precursor tris-dimethylaminoarsenic.[19]

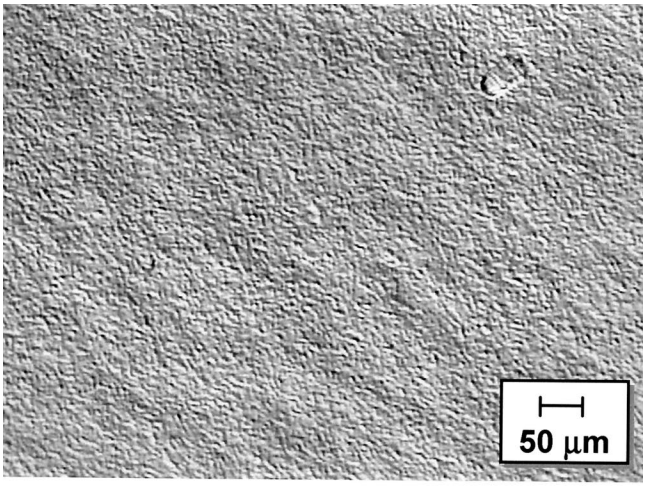

a

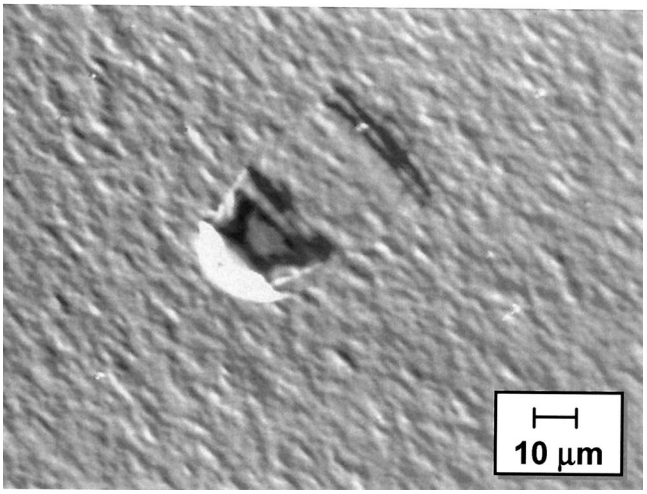

b

Fig. 1. Nomarski optical micrographs at two different magnifications of HgCdTe grown on (552)B oriented CdZnTe. The hillock (a) is the same one shown in (b) at greater magnification.

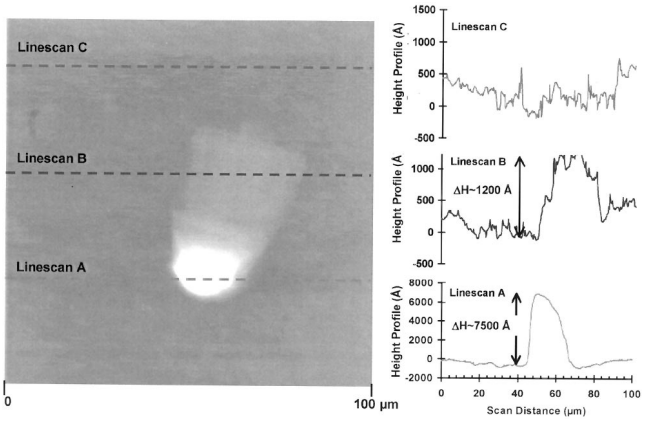

Fig. 2. AFM Image of a 100 μm × 100 μm area of (552)B HgCdTe.

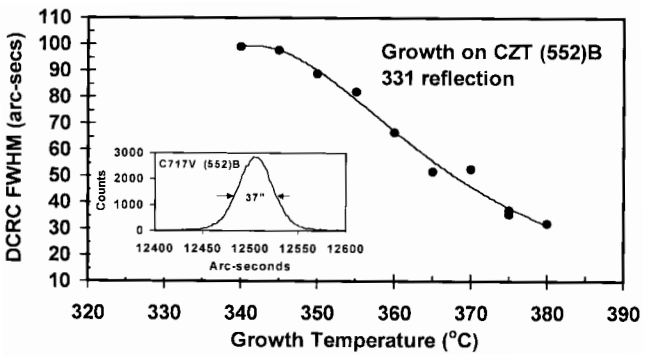

Fig. 3. X-ray double crystal rocking curve data on HgCdTe films grown on (552)B CdZnTe in the temperature range of 330–380°C.

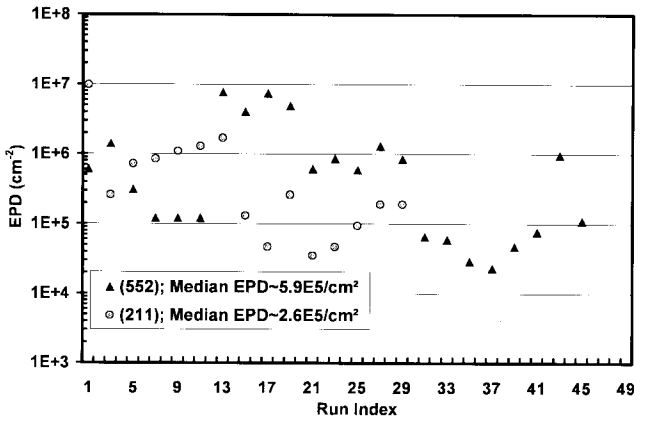

Fig. 4. Etch pit density data comparison between (552)B and (211)B oriented MOVPE HgCdTe grown in a number of runs.

SURFACE MORPHOLOGY AND DEFECTS

The surface of the HgCdTe grown on the (552)B-oriented CdZnTe exhibits hillock defects at a density of 10–50 cm^{-2}. Void defects, commonly observed on (211)B HgCdTe, however, are not observed. Figure 1 shows the Nomarski optical micrographs of a (552)B HgCdTe film that is 14 μm thick, at two different magnifications. The surface is relatively smooth and a bell-shaped hillock defect is visible. The hillock is ~55 μm long, ~30 μm wide, and has a higher elevation on one end. To obtain a quantitative height profile, the surface was imaged by atomic force microscopy (AFM). Figure 2 shows a 100 μm by 100 μm AFM scan of a hillock from another 12.5 μm thick (552)B film. A line scan of the tallest region of the hil-lock (region A) shows it to be ~7500 Å high and ~15 μm wide. The flatter region (region B) of the hillock is 1200 Å high and ~25 μm wide. In a hillock- free region the line scan (region C) shows the surface roughness to be ~400 Å.

Back reflection Laue x-ray diffraction patterns showed the HgCdTe epitaxial layer to be single crystal with (552) orientation. The Laue pattern showed no evidence of twinning. The Laue pattern of a (552)-oriented CdZnTe substrate matched the geometry of the HgCdTe pattern, confirming the film orientation.

A Bede 200 double-crystal diffractometer was used to investigate the x-ray ($CuK\alpha_1$) rocking curves of a number of (552)B HgCdTe films. The (331) reflection and a 1 mm spot size was used to measure the double crystal rocking curve (DCRC) full width at half maximum (FWHM). For films grown at 370–380°C the FWHM was found to be in the range of 30–40 arcsec. The presence of twinning on the (552) surface was studied by first locating the (331) reflection, then moving the detector and sample appropriately for a (422) reflection and rotating about the sample surface normal to locate any (422) reflection present. In most cases, there was no evidence of twinning. For films grown at 340–350°C a 1–3% twin volume was detected. These films also exhibit a relatively wider FWHM of 90–100 arcsec. Figure 3 shows a plot of the DCRC FWHM for (552)B films grown in the temperature range of 340–380°C. The narrowest FWHM are for films grown at 375–380°C with values of 30–35 arcsec.

The dislocations in the (552)B films were studied by etch pit density (EPD) counts using the Hahnert and Schenk dislocation revealing etch[20] (HF, HNO_3, H_2O, CrO_3). This etch was found to be effective in producing triangular pits on both A and B faces of the (552) HgCdTe films. The EPD counts for a number of (552)B and (211)B films are plotted in Fig. 4. The plot shows the run-to-run variation during the growth optimization process so all the films were not grown under identical conditions. The growth temperature in all cases was 380°C. The median EPD values for the 23 (552)B films and the 15 (211)B films are 5.9×10^5 and 2.6×10^5 cm^{-2}, respectively. The higher median EPD for the (552)B-oriented films is more due to the inclusion of the optimization runs rather than due to a fundamental limitation in obtaining EPD values comparable to the (211)B films. In fact, in six of the (552)B films the EPD is below 10^5 cm^{-2}, values that are comparable to the lowest EPD values in the (211)B films. These values are also comparable to state-of-the-art MBE and LPE grown single layer HgCdTe films.

EPD and the x-value depth profile of a multilayer P-n-N HgCdTe (552)B film is shown in Fig. 5. The p-type layer was doped with arsenic at 5×10^{16} cm^{-3}. The n-type buffer and absorber layers were doped with iodine at 4×10^{15} and 1×10^{15} cm^{-3}, respectively. The x-value depth profile was obtained by secondary ion mass spectrometry (SIMS) performed at Charles Evans

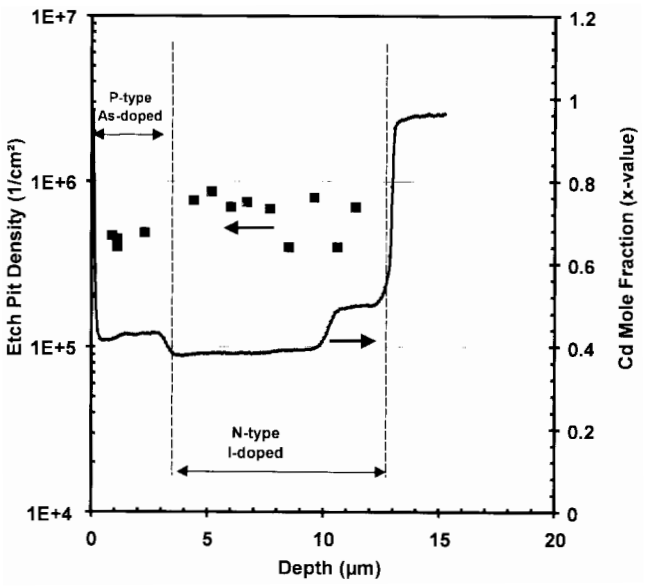

Fig. 5. EPD depth profile in a P-n-N HgCdTe film grown on a (552)B substrate.

& Associates. The EPD depth profile was measured on a differentially etched wedge from a 15 mm long strip of the film with thickness varying from 1 μm to the full film thickness of 13 μm. The wedge-film was then immersed in the etchant solution to reveal the dislocation pits with varying depths.[21] Figure 5 shows the EPD count to be uniform throughout the depth of the film with an average value of ~6×10^5 cm^{-2}. Thus for the range of x-values and doping levels of this multilayer film, increased EPD over single layer films are not observed.

TRANSPORT PROPERTIES

The Hall parameters of a number of n-type single layer (552)B HgCdTe films with x-values in the range of 0.20 to 0.43 were measured at 77 K and a magnetic field of 3.2 kgauss. For undoped films the background carrier concentrations are in the range of (1–3) × 10^{14} cm^{-3}. The 77 K mobility data for iodine-doped films, with carrier concentrations in the range of (0.5–2) × 10^{15} cm^{-3}, are plotted in Fig. 6. Also plotted for comparison are data from similar MOVPE (211)B-oriented films. Figure 6 shows that the mobility data for the (552)B and (211)B HgCdTe films are comparable and closely follow the trend line for recent Te-rich LPE grown HgCdTe at BAE SYSTEMS, Lexington, MA.

The iodine-doped (552)B n-type films were characterized for temperature dependent lifetimes by the non-contact transient mm-wave reflectance technique.[22] Inverse temperature dependent lifetimes for two long-wave infrared (LWIR) composition films (x ~ 0.23) with Hall carrier concentrations of 1.3×10^{15} and 1.8×10^{15} cm^{-3} are plotted in Fig. 7. Also plotted for comparison are model calculations for the temperature dependent lifetimes based on Auger-1 and radiative recombination at donor concentrations of 1×10^{15} and 2×10^{15} cm^{-3}. For the HgCdTe layer doped at 1.3×10^{15} cm^{-3} the lifetime is 0.80 μsec at 77 K and

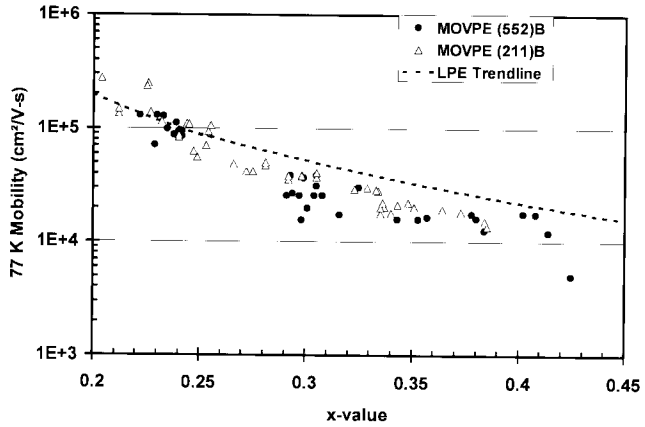

Fig. 6. Mobility of iodine doped MOVPE (552)B and (211)B HgCdTe and the trendline for LPE HgCdTe films of the same composition grown recently at BAE SYSTEMS, Lexington MA.

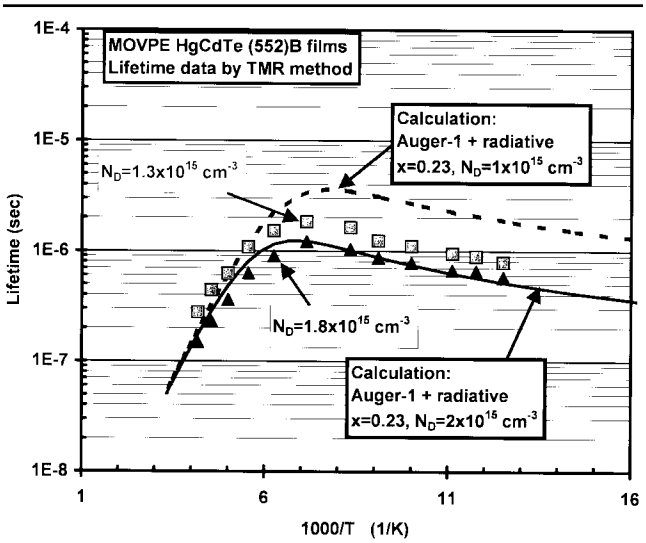

Fig. 7. Lifetimes of MOVPE LWIR (552)B oriented HgCdTe films grown with two different donor concentrations. The solid and dotted lines are model calculations based on the Auger-1 and radiative recombination processes for N_D-N_A of 2×10^{15} and 1×10^{15} cm^{-3}, respectively.

peaks at 1.85 μsec at 140 K. Figure 7 shows that the measured lifetimes fall within the calculated ranges for the two carrier concentrations.

DETECTOR ARRAY RESULTS

For characterizing the quality of detector performance an MWIR P-n-N heterojunction (552)B HgCdTe film was fabricated into back-illuminated, mesa-etched variable-area diagnostic photodiode arrays.[23] The test array consisted of 43 widely separated circular diodes with junction diameters ranging from 40 μm to 350 μm. It was indium bump-mounted to a circuit board and illuminated through the CdZnTe substrate. Spectral response was classical in shape with a cutoff wavelength of 5.22 μm at 120 K (Fig. 8). Quantum efficiency was measured using a calibrated 1000 K blackbody and a narrow-band filter at 3.0 μm. From the area dependence of detector responsivity, a 1-dimensional quantum efficiency of 78% and a lateral collection length of 38 μm were determined. The quantum efficiency is within experimental accuracy of the 79%

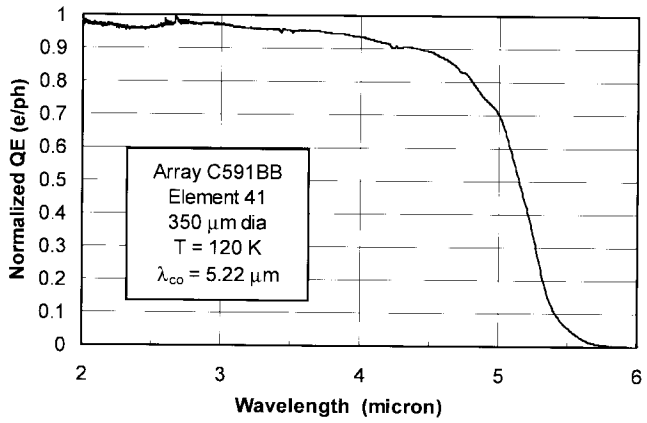

Fig. 8. Normalized quantum efficiency as a function of wavelength.

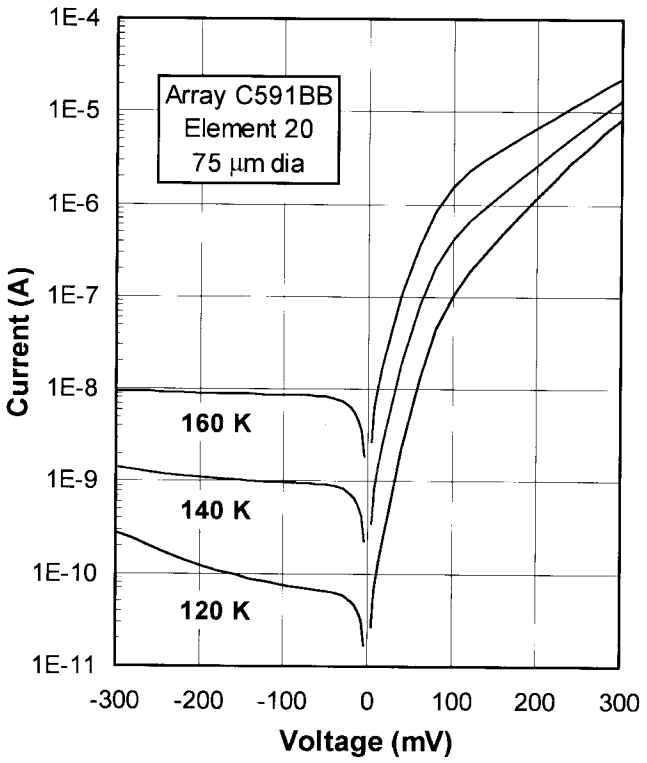

Fig. 9. Current-voltage characteristics at three temperatures.

limit imposed by reflection from the uncoated CdZnTe substrate surface, implying nearly 100% internal quantum efficiency. Figures 9 and 10 show the current-voltage and resistance-voltage characteristics of one of the diodes at temperatures ranging from 120 K to 160 K. The exponential voltage dependence with a junction ideality factor of 1 and the temperature dependence of R_0A both indicate diffusion current is the dominant mechanism near zero bias. The impedance increases by more than a factor of 30 at reverse bias, important for minimizing noise when the detectors are used with a silicon multiplexer in a focal plane array (FPA). Tunneling current, apparent at large reverse bias at lower temperatures, is not significant at the reverse bias of –20 mV typical of FPA operation. The dynamic resistance-area RA_{opt} products at 0 and –40 mV bias voltage for a temperature

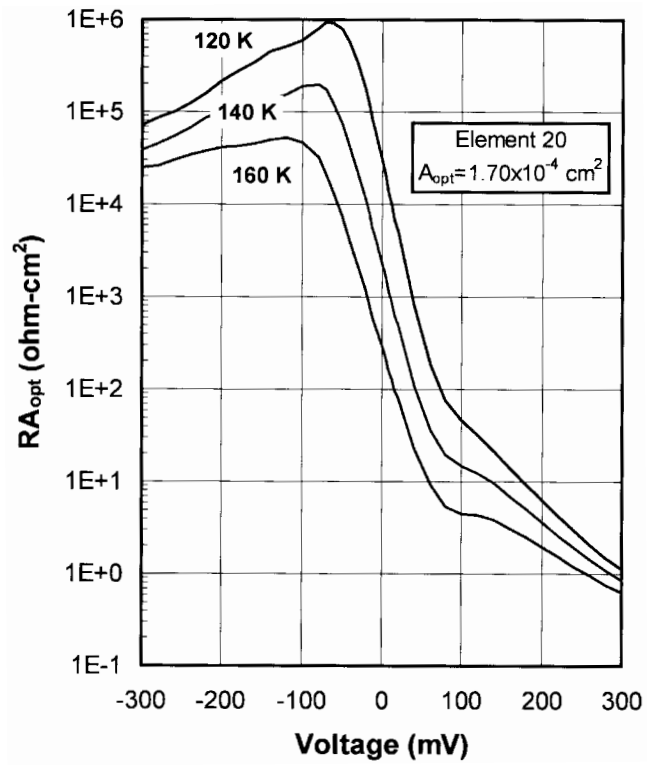

Fig. 10. Resistance-area product as a function of bias and temperature.

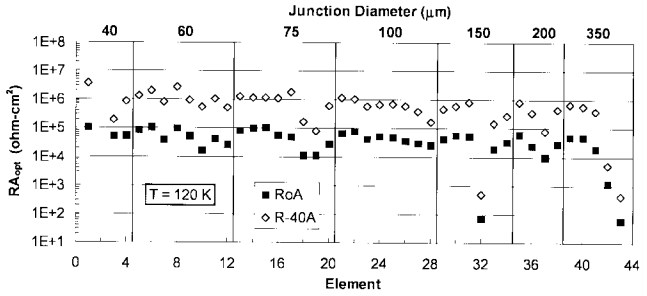

Fig. 11. Resistance-area product, using the optically active area, for all elements of the test array. R_0A is measured at zero bias and R-40A is measured at –40 mV.

of 120 K are shown for all detectors in the array in Fig. 11. The optical area, A_{opt}, is defined as the area plus an annulus of width equal to the lateral collection length. High R_0A values, up to 1×10^5 ohm-cm^2, and large impedance improvements at reverse bias are seen for nearly all detectors. The three detectors with R-40A value less than 10^4 ohm-cm^2 all had large hillock defects in the HgCdTe material. These defects were localized at one end of the array. The near independence of RA_{opt} with detector size is another indication that diffusion current from the n-type absorber layer determines R_0A in these devices.

DISCUSSION AND CONCLUSIONS

MOVPE HgCdTe films on (552)B-oriented CdZnTe exhibit smooth surface morphology with short bell-shaped hillocks and no void defects. For films as thick as 14 μm the hillocks at their tallest point are no higher than 7500 Å. In its flatter region the hillock is only 1200 Å high. The surface morphology is similar

to that of the off-axis (100) MOVPE HgCdTe films, which exhibit much taller pyramidal-shaped hillocks, and also no void defects. An off-axis (100) HgCdTe film that is ~14 μm thick exhibits hillocks that are significantly larger (60–80 μm long) and taller (4–7 μm). The hillock density in a (552)B film is typically in the range of 10–50 cm^{-2}. Assuming that a hillock would cause outages on all photodiode pixels delineated in that area, the reduction in FPA operability is not very significant. For a 256 × 256 FPA with 40 μm pitch pixels, a hillock density of 50 cm^{-2} would cause only 0.23% of the pixels to be out, if each hillock causes 3 pixels to be defective. In off-axis (100) HgCdTe films the same density of hillocks as in (552)B HgCdTe would cause a larger number of pixel outages. During patterning of the (100) HgCdTe films by photolithography the larger and taller hillocks cause the photoresist to bead around them affecting a wider area, and thus a larger number of pixels. Thus, purely from the standpoint of outages caused by macrodefects, higher operability is expected for FPAs fabricated on (552)B HgCdTe films.

The x-ray DCRC FWHM of the (552) HgCdTe with the (331) reflection is in the range of 30–40 arcsec, values similar to those obtained in high quality epitaxial HgCdTe films. EPD counts on the films grown with optimized growth parameters are found to be in the range of high 10^4 to mid 10^5 cm^{-2}, which are comparable to the counts obtained on (211)B MOVPE HgCdTe, and are also similar to state-of-the-art epitaxial HgCdTe grown by MBE and LPE. In (552)B multilayer structures grown in the P-n-N configuration, the dislocation density is found to be relatively constant, independent of film depth and doping type.

The electrical transport properties of the (552)B HgCdTe films are similar to those measured on (211)B MOVPE HgCdTe. The background doping level, mobilities of iodine-doped films, and carrier lifetimes are all found to be very similar for the (552)B and (211)B orientations, and closely follow state-of-the-art data for LPE HgCdTe. Backside-illuminated MWIR detectors fabricated from (552)B P-n-N heterojunction films exhibit characteristics that closely match the performance of similar (211)B films. The R_0A values at 140 K are within a factor of two of the one-dimensional diffusion current model calculation,[6] and the quantum efficiency value of 78% is at the limit imposed by reflection losses at the non-antireflection-coated CdZnTe substrate surface. The dark current near zero-bias voltage is limited by diffusion current, and the spectral response is classical. Those detectors whose junction areas overlap the bell-shaped hillocks on the films have significantly lower R_0A values (by two or three orders of magnitude) along with lower quantum efficiency (QE) and higher reverse-bias dark current. The low density (10–50 cm^{-2}) of these macrodefects, however, will result in relatively few outages in two-dimensional detector arrays. Based on the hillock densities and their sizes, FPAs with 30–40 μm pitch detectors are expected to have outages in the range of 0.10–0.25%. These estimates of defective pixel counts would result in significant improvement in FPA operability than the current standard based on (211)B films grown by vapor phase epitaxy.

ACKNOWLEDGEMENTS

This work was supported by the U.S. Army Space and Missile Defense Command Contract, monitored by Dr. Latika Becker; and by Lockheed Martin internal R&D funds. We thank L.C. Johnson and A.X. Quinonez for their contributions to the MOVPE growth experiments, P. Bodie for EPD measurements on the CZT substrates, and Dr. M.B. Reine for his valuable comments on the manuscript.

REFERENCES

1. S.J.C. Irvine, *Narrow-Gap II-VI Compounds for Optoelectronic and Electromagnetic Applications,* ed. P. Capper (London: Chapman & Hall, 1997), pp. 71–96.
2. P. Mitra, S.L. Barnes, F.C. Case, M.B. Reine, P. O'Dette, R. Starr, A. Hairston, K. Kuhler, M.H. Weiler, and B.L. Musicant, *J. Electron. Mater.* 26, 482 (1997).
3. C.D. Maxey, C.L. Jones, N.E. Metcalfe, R.A. Catchpole, N.T. Gordon, A.M. White, and C.T. Elliot, *SPIE Proc.* 3122, 453 (1997).
4. M.B. Reine, A. Hairston, P. O'Dette, S.P. Tobin, F.T.J. Smith, B.L. Musicant, P. Mitra, and F. C. Case, *SPIE Proc.* 3379, 200 (1998).
5. P. Mitra, F.C. Case, and M.B. Reine, *J. Electron. Mater.* 27, 510 (1998).
6. P. Mitra, F.C. Case, M.B. Reine, T. Parodos, S.P. Tobin, and P.W. Norton, *J. Electron. Mater.* 28, 589 (1999).
7. C.D. Maxey, M.U. Ahmed, C.L. Jones, R. A. Catchpole, P. Capper, N.T. Gordon, M. Houlton and T. Ashley (Paper presented at the 2000 U.S. Workshop on the Physics and Chemistry of II-VI Materials, Albuquerque, NM Oct. 30–Nov. 1, 2000).
8. P. Capper, C.D. Maxey, P.A.C. Whiffin and B.C. Easton, *J. Cryst. Growth* 96, 519 (1989).
9. G. Cinader, A. Raizman, and A. Sher, *J. Vac. Sci. Technol.* B9, 1634 (1991).
10. M.J. Bevan, N.J. Doyle, and T.A. Temofonte, *J. Appl. Phys.* 71, 204 (1992).
11. R. Triboulet, A. Tromson-Carli, D. Lorans, and T. Nguyen Duy, *J. Electron. Mater.* 22, 827 (1993).
12. J. Geiss, J.E. Hails, A. Graham, G. Blackmore, M.R. Houlton, J. Newey, M.L. Young, M.G. Astles, W. Bell, and D.J. Cole-Hamiliton, *J. Electron. Mater.* 24 1149 (1995).
13. S.-H. Suh, J.-H. Song, and S.-W. Moon, *J. Cryst. Growth* 159, 1132 (1996).
14. J.E. Hails, D.J. Cole-Hamilton, and J. Geiss, *J. Electron. Mater.* 27, 624 (1998).
15. T.H. Meyers, J.F. Schetzina, T.J. Magee, and R.D. Ormond, *J. Vac. Sci. Technol.* A3, 1598 (1983).
16. W.J. Everson, C.K. Ard, J.L. Sepich, B.E. Dean, and H.F. Schaake, *J. Electron. Mater.* 24, 505 (1995).
17. P. Mitra, Y.L. Tyan, T.R. Schimert, and F.C. Case, *Appl. Phys. Lett.* 65, 195 (1994).
18. P. Mitra, F. C. Case, M. B. Reine, R. Starr and M. H. Weiler, *J. Cryst. Growth* 170, 542 (1997).
19. P. Mitra, Y.L. Tyan, F.C. Case, R. Starr, and M.B. Reine, *J. Electron. Mater.* 25, 1328 (1996).
20. I. Hahnert and M. Schenk, J. Cryst. Growth 101, 251 (1990).
21. P. Mitra, F.C. Case, S.L. Barnes, M.B. Reine, P. O'Dette, and S.P. Tobin, *Mater. Res. Soc. Symp. Proc.* 484, 233 (1998).
22. A.J. Brouns, T.R. Schimert, P. Mitra, F.C. Case, S.L. Barnes, and Y.L. Tyan, *Semicond. Sci. Technol.* 8, 928 (1993).
23. M.B. Reine, K.R. Maschhoff, S.P. Tobin, P.W. Norton, J.A. Mroczkowski, and E.E. Krueger, *Semicond. Sci. Technol.* 8, 788 (1993).